

Chapter 9: PD Controller

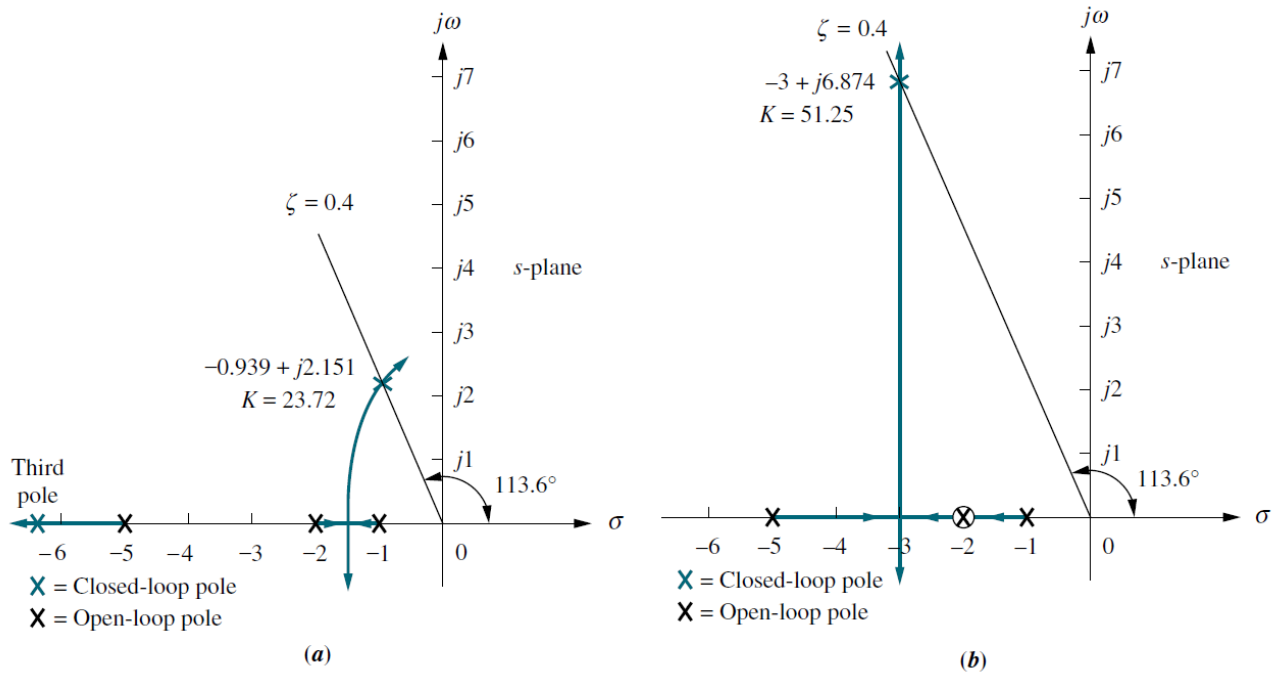


FIGURE 9.15 Using ideal derivative compensation: **a.** uncompensated; **b.** compensator zero at -2 ; (figure continues)

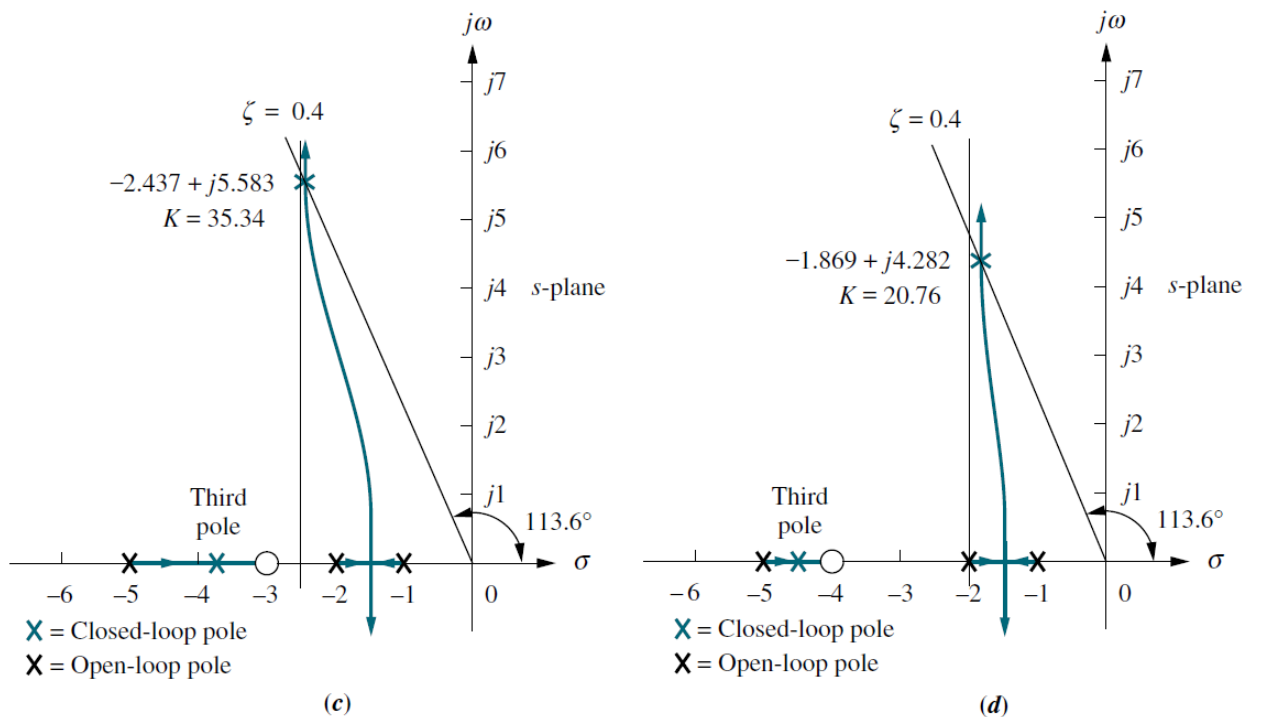


FIGURE 9.15 (Continued) **c.** compensator zero at -3 ; **d.** compensator zero at -4 .

TABLE 9.2 Predicted characteristics for the systems of Figure 9.15

	Uncompensated	Compensation b	Compensation c	Compensation d
Plant and compensator	$\frac{K}{(s+1)(s+2)(s+5)}$	$\frac{K(s+2)}{(s+1)(s+2)(s+5)}$	$\frac{K(s+3)}{(s+1)(s+2)(s+5)}$	$\frac{K(s+4)}{(s+1)(s+2)(s+5)}$
Dom. poles	$-0.939 \pm j2.151$	$-3 \pm j6.874$	$-2.437 \pm j5.583$	$-1.869 \pm j4.282$
K	23.72	51.25	35.34	20.76
ζ	0.4	0.4	0.4	0.4
ω_n	2.347	7.5	6.091	4.673
%OS	25.38	25.38	25.38	25.38
T_s	4.26	1.33	1.64	2.14
T_p	1.46	0.46	0.56	0.733
K_p	2.372	10.25	10.6	8.304
$e(\infty)$	0.297	0.089	0.086	0.107
Third pole	-6.123	None	-3.127	-4.262
Zero	None	None	-3	-4
Comments	Second-order approx. OK	Pure second-order	Second-order approx. OK	Second-order approx. OK

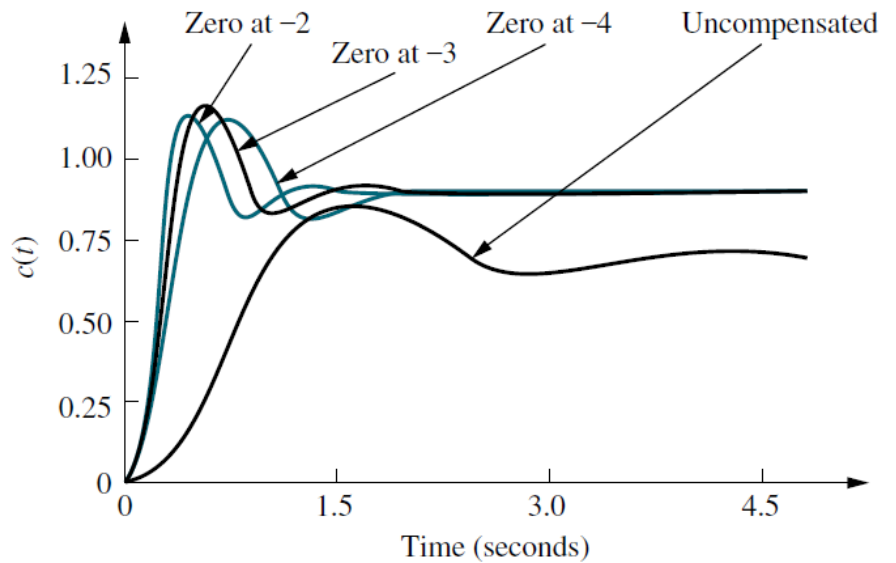


FIGURE 9.16 Uncompensated system and ideal derivative compensation solutions from Table 9.2

Example 9.5

PID Controller Design

PROBLEM: Given the system of Figure 9.31, design a PID controller so that the system can operate with a peak time that is two-thirds that of the uncompensated system at 20% overshoot and with zero steady-state error for a step input.

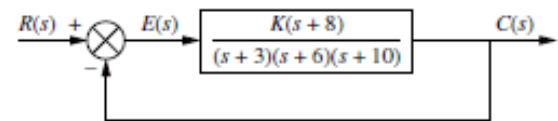


FIGURE 9.31 Uncompensated feedback control system for Example 9.5

SOLUTION: Note that our solution follows the eight-step procedure described earlier.

Step 1 Let us first evaluate the uncompensated system operating at 20% overshoot. Searching along the 20% overshoot line ($\zeta = 0.456$) in Figure 9.32, we find the dominant poles to be $-5.415 \pm j10.57$ with a gain of 121.5. A third pole, which exists at -8.169 , is found by searching the region

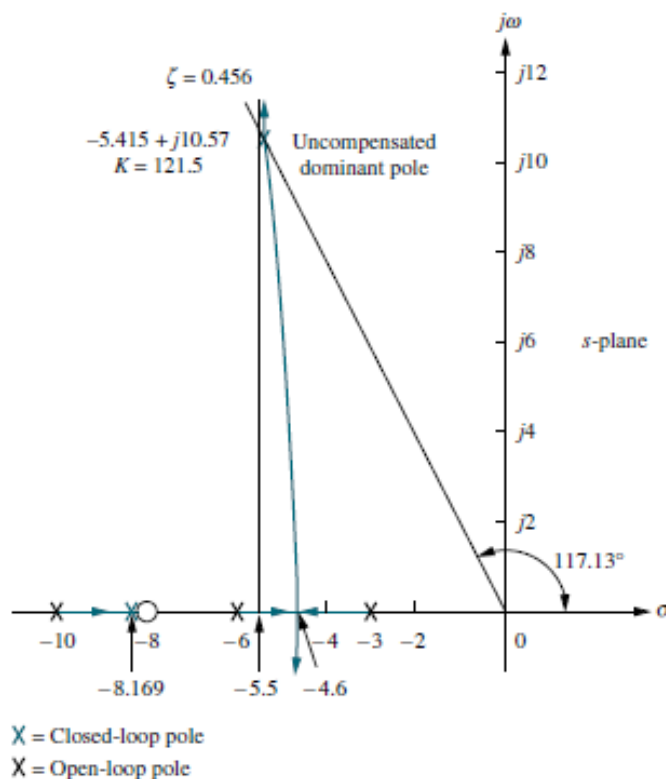


FIGURE 9.32 Root locus for the uncompensated system of Example 9.5

TABLE 9.5 Predicted characteristics of uncompensated, PD-, and PID-compensated systems of Example 9.5

	Uncompensated	PD-compensated	PID-compensated
Plant and compensator	$\frac{K(s+8)}{(s+3)(s+6)(s+10)}$	$\frac{K(s+8)(s+55.92)}{(s+3)(s+6)(s+10)}$	$\frac{K(s+8)(s+55.92)(s+0.5)}{(s+3)(s+6)(s+10)s}$
Dominant poles	$-5.415 \pm j10.57$	$-8.13 \pm j15.87$	$-7.516 \pm j14.67$
K	121.5	5.34	4.6
ζ	0.456	0.456	0.456
ω_n	11.88	17.83	16.49
%OS	20	20	20
T_s	0.739	0.492	0.532
T_p	0.297	0.198	0.214
K_p	5.4	13.27	∞
$e(\infty)$	0.156	0.070	0
Other poles	-8.169	-8.079	-8.099, -0.468
Zeros	-8	-8, -55.92	-8, -55.92, -0.5
Comments	Second-order approx. OK	Second-order approx. OK	Zeros at -55.92 and -0.5 not canceled

between -8 and -10 for a gain equivalent to that at the dominant poles. The complete performance of the uncompensated system is shown in the first column of Table 9.5, where we compare the calculated values to those obtained through simulation (Figure 9.35). We estimate that the uncompensated system has a peak time of 0.297 second at 20% overshoot.

Step 2 To compensate the system to reduce the peak time to two-thirds of that of the uncompensated system, we must first find the compensated system's dominant pole location. The imaginary part of the compensated dominant pole is

$$\omega_d = \frac{\pi}{T_p} = \frac{\pi}{(2/3)(0.297)} = 15.87 \quad (9.22)$$

Thus, the real part of the compensated dominant pole is

$$\sigma = \frac{\omega_d}{\tan 117.13^\circ} = -8.13 \quad (9.23)$$

Next we design the compensator. Using the geometry shown in Figure 9.33, we calculate the compensating zero's location. Using the root locus program, we find the sum of angles from the uncompensated system's poles and zeros to the desired compensated dominant pole to be -198.37° . Thus, the contribution required from the compensator zero is $198.37^\circ - 180^\circ = 18.37^\circ$. Assume that the compensator zero is located at $-z_c$, as shown in Figure 9.33. Since

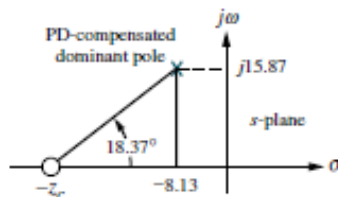
$$\frac{15.87}{z_c - 8.13} = \tan 18.37^\circ \quad (9.24)$$

then

$$z_c = 55.92 \quad (9.25)$$

Thus, the PD controller is

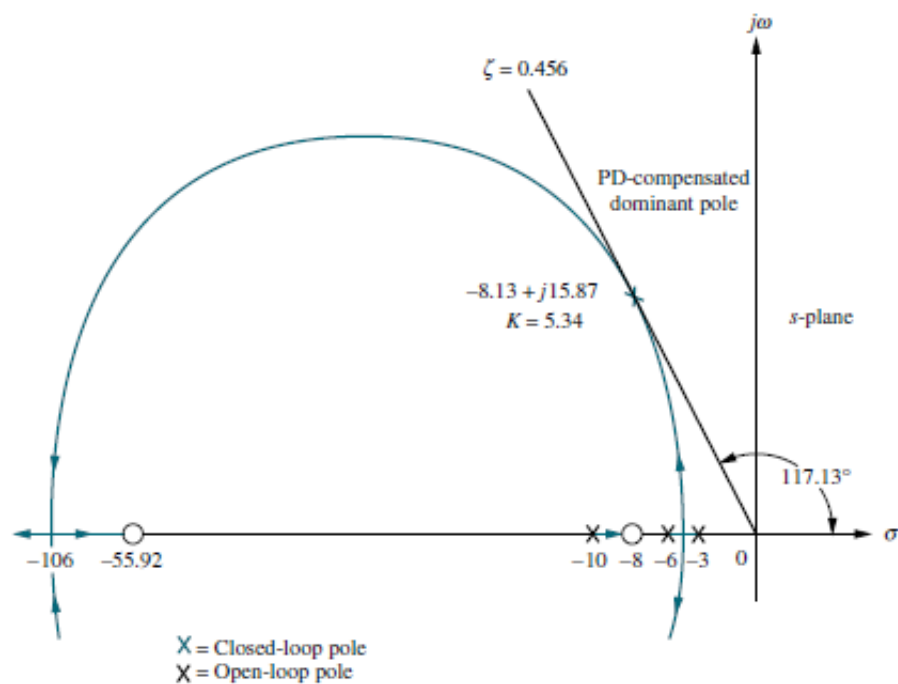
$$G_{PD}(s) = (s + 55.92) \quad (9.26)$$



X = Closed-loop pole

Note: This figure is not drawn to scale.

FIGURE 9.33 Calculating the PD compensator zero for Example 9.5



Note: This figure is not drawn to scale.

FIGURE 9.34 Root locus for PD-compensated system of Example 9.5

The complete root locus for the PD-compensated system is sketched in Figure 9.34. Using a root locus program, the gain at the design point is 5.34. Complete specifications for ideal derivative compensation are shown in the third column of Table 9.5.

Steps 3 and 4 We simulate the PD-compensated system, as shown in Figure 9.35.

We see the reduction in peak time and the improvement in steady-state error over the uncompensated system.

Step 5 After we design the PD controller, we design the ideal integral compensator to reduce the steady-state error to zero for a step input. Any ideal integral compensator zero will work, as long as the zero is placed close to the origin. Choosing the ideal integral compensator to be

$$G_{PI}(s) = \frac{s + 0.5}{s} \quad (9.27)$$

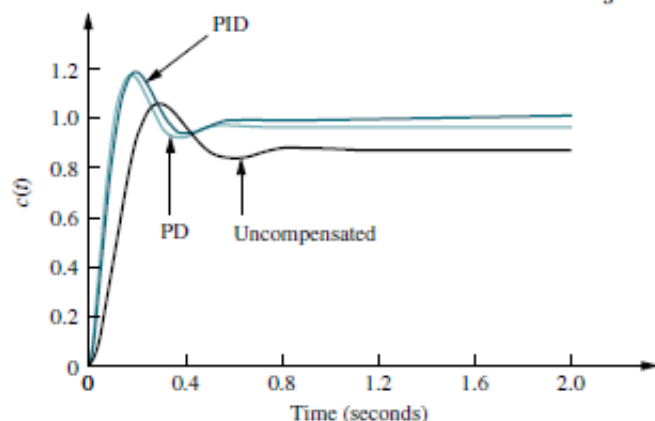
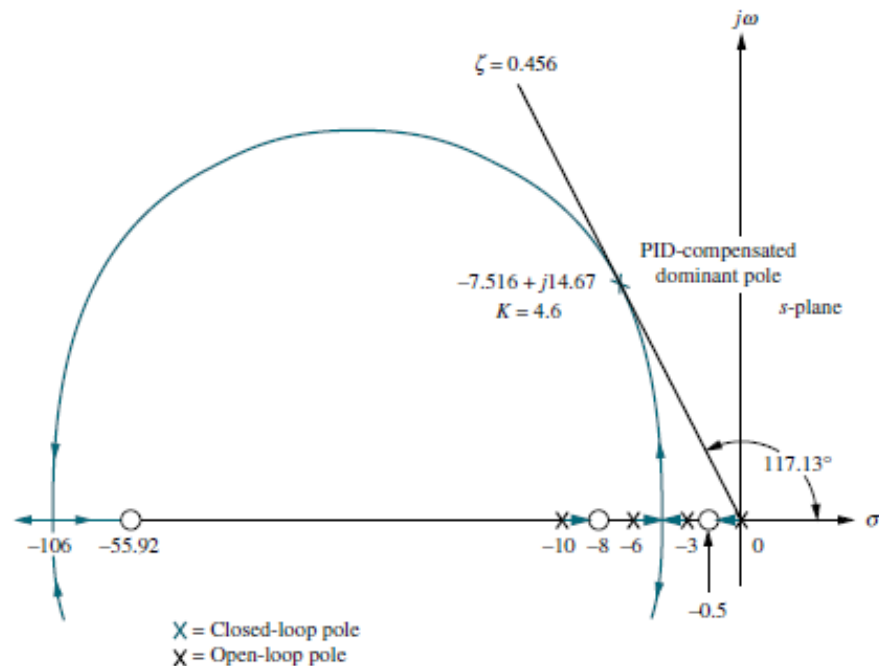


FIGURE 9.35 Step responses for uncompensated, PD-compensated, and PID-compensated systems of Example 9.5



Note: This figure is not drawn to scale.

FIGURE 9.36 Root locus for PID-compensated system of Example 9.5

we sketch the root locus for the PID-compensated system, as shown in Figure 9.36. Searching the 0.456 damping ratio line, we find the dominant, second-order poles to be $-7.516 \pm j14.67$, with an associated gain of 4.6. The remaining characteristics for the PID-compensated system are summarized in the fourth column of Table 9.5.

Step 6 Now we determine the gains, K_1, K_2 , and K_3 , in Figure 9.30. From Eqs. (9.26) and (9.27), the product of the gain and the PID controller is

$$\begin{aligned}
 G_{\text{PID}}(s) &= \frac{K(s + 55.92)(s + 0.5)}{s} = \frac{4.6(s + 55.92)(s + 0.5)}{s} \\
 &= \frac{4.6(s^2 + 56.42s + 27.96)}{s}
 \end{aligned} \tag{9.28}$$

Matching Eqs. (9.21) and (9.28), $K_1 = 259.5$, $K_2 = 128.6$, and $K_3 = 4.6$

Steps 7 and 8 Returning to Figure 9.35, we summarize the results of our design. PD compensation improved the transient response by decreasing the time required to reach the first peak as well as yielding some improvement in the steady-state error. The complete PID controller further improved the steady-state error without appreciably changing the transient response designed with the PD controller. As we have mentioned before, the PID controller exhibits a slower response, reaching the final value of unity at approximately 3 seconds. If this is undesirable, the speed of the system must be increased by redesigning the ideal derivative compensator or moving the PI controller zero farther from the origin. Simulation plays an important role in this type of design since our derived equation for settling time is not applicable for this part of the response, where there is a slow correction of the steady-state error.

Example 9.6

Lag-Lead Compensator Design

PROBLEM: Design a lag-lead compensator for the system of Figure 9.37 so that the system will operate with 20% overshoot and a twofold reduction in settling time. Further, the compensated system will exhibit a tenfold improvement in steady-state error for a ramp input.

SOLUTION: Again, our solution follows the steps just described.

Step 1 First we evaluate the performance of the uncompensated system. Searching along the 20% overshoot line ($\zeta = 0.456$) in Figure 9.38, we find the dominant poles at $-1.794 \pm j3.501$, with a gain of 192.1. The performance of the uncompensated system is summarized in Table 9.6.

Step 2 Next we begin the lead compensator design by selecting the location of the compensated system's dominant poles. In order to realize a twofold reduction in settling time, the real part of the dominant pole must be increased by a factor of 2, since the settling time is inversely proportional to the real part. Thus,

$$-\zeta\omega_n = -2(1.794) = -3.588 \quad (9.29)$$

The imaginary part of the design point is

$$\omega_d = \zeta\omega_n \tan 117.13^\circ = 3.588 \tan 117.13^\circ = 7.003 \quad (9.30)$$

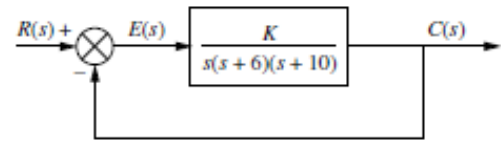


FIGURE 9.37 Uncompensated system for Example 9.6

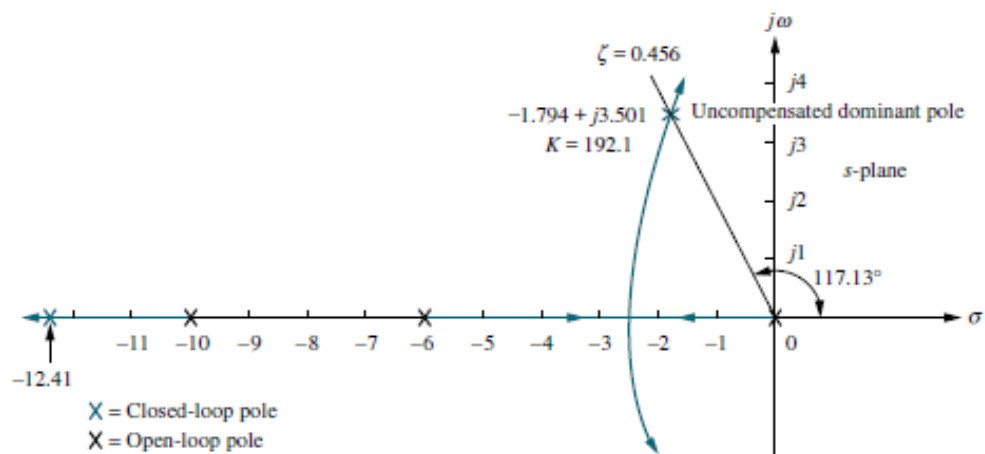


FIGURE 9.38 Root locus for uncompensated system of Example 9.6

Now we design the lead compensator. Arbitrarily select a location for the lead compensator zero. For this example, we select the location of the compensator zero coincident with the open-loop pole at -6 . This choice will eliminate a zero and leave the lead-compensated system with three poles, the same number that the uncompensated system has.

We complete the design by finding the location of the compensator pole. Using the root locus program, sum the angles to the design point from the uncompensated system's poles and zeros and the compensator zero and get -164.65° . The difference between 180° and this quantity is the angular contribution required from the compensator pole, or -15.35° . Using the geometry shown in Figure 9.39,

$$\frac{7.003}{p_c - 3.588} = \tan 15.35^\circ \quad (9.31)$$

from which the location of the compensator pole, p_c , is found to be -29.1 .

TABLE 9.6 Predicted characteristics of uncompensated, lead-compensated, and lag-lead-compensated systems of Example 9.6

	Uncompensated	Lead-compensated	Lag-lead-compensated
Plant and compensator	$\frac{K}{s(s+6)(s+10)}$	$\frac{K}{s(s+10)(s+29.1)}$	$\frac{K(s+0.04713)}{s(s+10)(s+29.1)(s+0.01)}$
Dominant poles	$-1.794 \pm j3.501$	$-3.588 \pm j7.003$	$-3.574 \pm j6.976$
K	192.1	1977	1971
ζ	0.456	0.456	0.456
ω_n	3.934	7.869	7.838
%OS	20	20	20
T_s	2.230	1.115	1.119
T_p	0.897	0.449	0.450
K_v	3.202	6.794	31.92
$e(\infty)$	0.312	0.147	0.0313
Third pole	-12.41	-31.92	$-31.91, -0.0474$
Zero	None	None	-0.04713
Comments	Second-order approx. OK	Second-order approx. OK	Second-order approx. OK

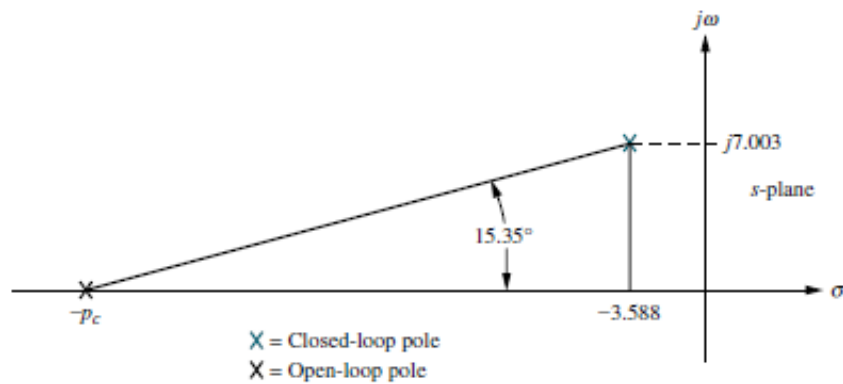


FIGURE 9.39 Evaluating the compensator pole for Example 9.6

The complete root locus for the lead-compensated system is sketched in Figure 9.40. The gain setting at the design point is found to be 1977.

Steps 3 and 4 Check the design with a simulation. (The result for the lead-compensated system is shown in Figure 9.42 and is satisfactory.)

Step 5 Continue by designing the lag compensator to improve the steady-state error. Since the uncompensated system's open-loop transfer function is

$$G(s) = \frac{192.1}{s(s+6)(s+10)} \quad (9.32)$$

the static error constant, K_v , which is inversely proportional to the steady-state error, is 3.201. Since the open-loop transfer function of the lead-compensated system is

$$G_{LC}(s) = \frac{1977}{s(s+10)(s+29.1)} \quad (9.33)$$

the static error constant, K_v , which is inversely proportional to the steady-state error, is 6.794. Thus, the addition of lead compensation has improved the steady-state error by a factor of 2.122. Since the requirements of the problem specified a tenfold improvement, the lag compensator must be designed to improve the steady-state error by a factor of 4.713 ($10/2.122 = 4.713$) over the lead-compensated system.

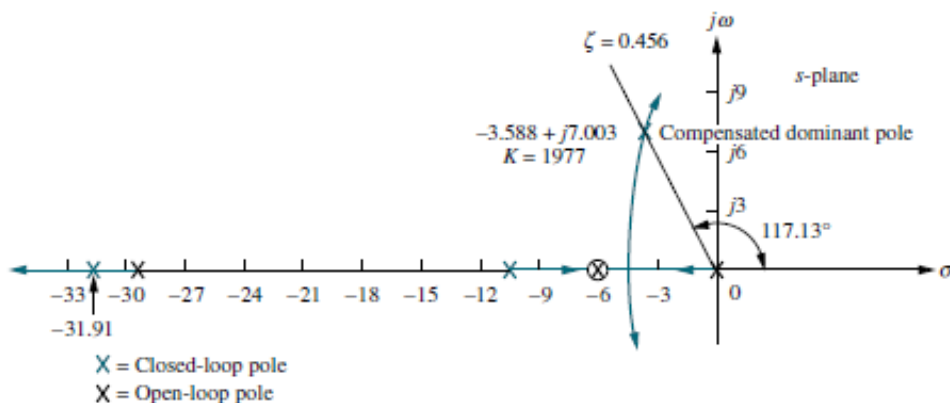
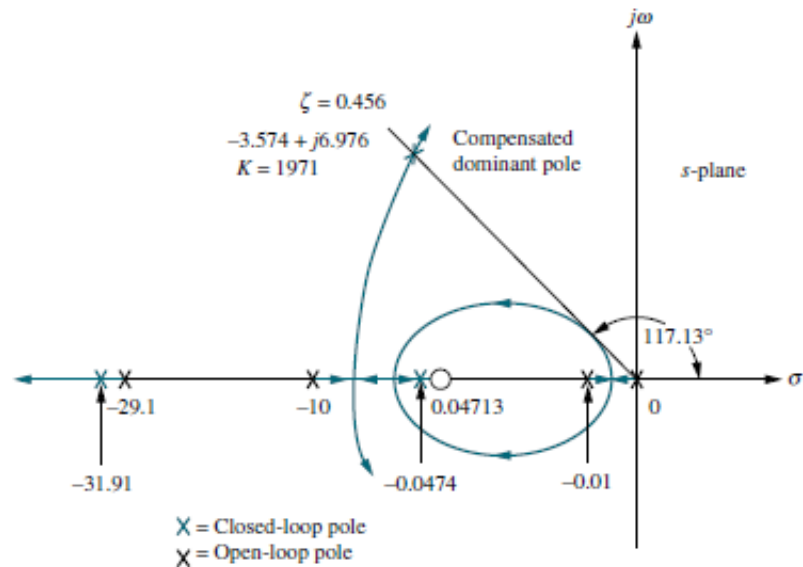


FIGURE 9.40 Root locus for lead-compensated system of Example 9.6



Note: This figure is not drawn to scale.

FIGURE 9.41 Root locus for lag-lead-compensated system of Example 9.6

Step 6 We arbitrarily choose the lag compensator pole at 0.01, which then places the lag compensator zero at 0.04713, yielding

$$G_{\text{lag}}(s) = \frac{(s + 0.04713)}{(s + 0.01)} \quad (9.34)$$

as the lag compensator. The lag-lead-compensated system's open-loop transfer function is

$$G_{\text{LLC}}(s) = \frac{K(s + 0.04713)}{s(s + 10)(s + 29.1)(s + 0.01)} \quad (9.35)$$

where the uncompensated system pole at -6 canceled the lead compensator zero at -6 . By drawing the complete root locus for the lag-lead-compensated system and by searching along the 0.456 damping ratio line, we find the dominant, closed-loop poles to be at $-3.574 \pm j6.976$, with a gain of 1971. The lag-lead-compensated root locus is shown in Figure 9.41.

A summary of our design is shown in Table 9.6. Notice that the lag-lead compensation has indeed increased the speed of the system, as witnessed by the settling time or the peak time. The steady-state error for a ramp input has also decreased by about 10 times, as seen from $e(\infty)$.

Step 7 The final proof of our designs is shown by the simulations of Figures 9.42 and 9.43. The improvement in the transient response is shown in Figure 9.42, where we see the peak time occurring sooner in the lag-lead-compensated system. Improvement in the steady-state error for a ramp input is seen in Figure 9.43, where each step of our design yields more improvement. The improvement for the lead-compensated system is shown in Figure 9.43(a), and the final improvement due to the addition of the lag is shown in Figure 9.43(b).

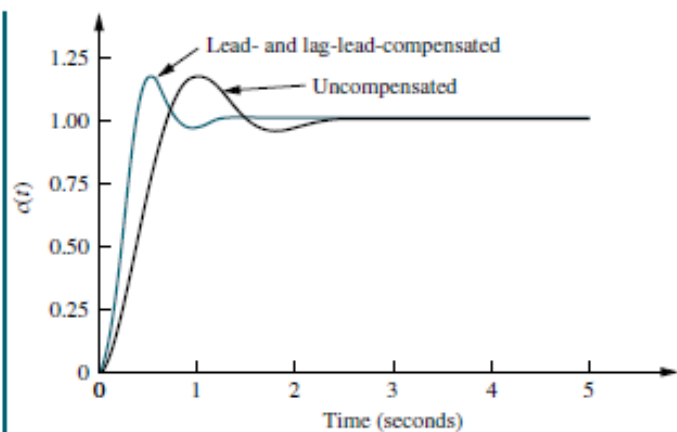


FIGURE 9.42 Improvement in step response for lag-lead-compensated system of Example 9.6

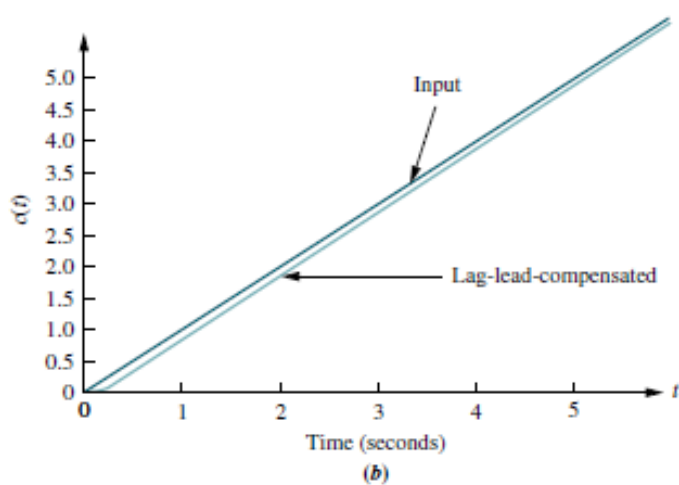
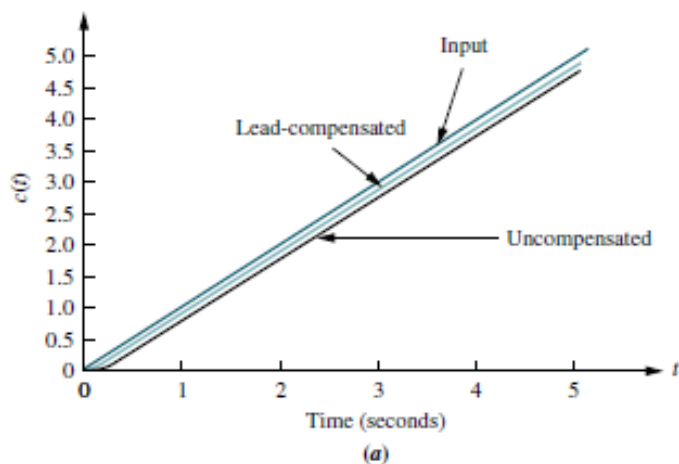


FIGURE 9.43 Improvement in ramp response error for the system of Example 9.6:
a. lead-compensated;
b. lag-lead-compensated